

On the Uniqueness of Solutions in GPS Source Localization: Distance and Squared-Distance Minimization under Limited Measurements in Two and Three Dimensions

Kiwoon KWON*

March 2, 2026

Abstract

The source localization problem, fundamental to applications like GPS, is typically approached as a minimization problem in the presence of various types of noise. Ensuring the uniqueness of solutions in GPS technology is vital for the reliability and accuracy of applications, from everyday navigation to critical military operations. In this paper, we examine two key minimization problems: one focused on distance error and the other on squared distance error. We explore these problems in both three-dimensional space, the standard scenario, and in two-dimensional space as a simplified case. Furthermore, we discuss the number of possible source solutions when the number of measurements is fewer than three. AMS: KEY WORDS: GPS, source localization, minimization

1 Introduction

The uniqueness of the source localization problem in Global Positioning System (GPS) technology is a fundamental aspect that ensures the reliability and accuracy of various applications, ranging from everyday navigation to critical military operations. This paper explores key issues related to the uniqueness of source localization and its implications for the stability and performance of GPS systems.

A central challenge in source localization is accurately and uniquely determining the position of a signal emitter despite the presence of noise, multipath effects, and other environmental factors. Multipath propagation, where GPS signals reflect off surfaces such as buildings and terrain, can introduce significant errors and ambiguities in position estimation. This issue is particularly severe in urban and densely built environments, leading to potential misidentification of the true signal source.

Another key factor is satellite geometry, the geometric configuration of the satellites in view. Poor satellite geometry can lead to weak geometric dilution of precision (GDOP), making it difficult to achieve unique and precise localization, especially in environments with limited satellite visibility, such as deep urban canyons or densely forested areas. Furthermore, precise time synchronization between the GPS satellites and the receiver is critical, as discrepancies in clock synchronization can introduce errors that compromise the uniqueness and accuracy of the localization process. Synchronizing time accurately across multiple satellites and receivers is a technical challenge that requires advanced algorithms and error correction techniques.

Additionally, the presence of multiple potential signal sources can complicate the localization process. Distinguishing between these sources and accurately identifying the correct one is essential for maintaining the stability and reliability of the GPS system, necessitating sophisticated signal processing techniques and robust algorithms capable of handling complex scenarios with overlapping signals.

*Department of Mathematics, Dongguk University-Seoul, 04620 Seoul, South Korea. e-mail address:kwkwon@dongguk.edu

In this paper, we investigate the conditions under which the proposed minimization problems yield unique solutions, particularly when the number of measurements is fewer than three. This aspect is crucial, as fewer than three measurements can make the problem significantly more challenging, leading to potential ambiguities and non-uniqueness in the solution. Understanding how this limitation impacts the problem and identifying strategies to address it are key contributions of this work.

We formulate the source localization problem as follows: Let $Z_i \in \mathbb{R}^n$ (with $n = 2$ or $n = 3$ represent the location of the i -th sensor ($i = 1, \dots, I$ for $I = 1, 2, 3$), and let $d_i \geq 0$ denote the measured distance between the source and the i -th sensor. The goal is to determine X , the location that minimizes the sum of the additive noise, expressed as:

$$X = \operatorname{argmin}_{\tilde{W}} O(\tilde{W}) = \{W \in \mathbb{R}^2 \text{ or } \mathbb{R}^3 | O(W) = \min_{\tilde{W}} O(\tilde{W})\}, \quad O(W) = \sum_{j=1}^I |\psi(\|W - Z_j\|) - \psi(d_j)| \quad (1)$$

where ψ is a non-negative, continuous, increasing function defined on $[0, \infty)$, vanishing only at zero. In this paper, we specifically consider the cases $\psi(y) = y$ and $\psi(y) = y^2$, which is called in this paper ‘distance error’ and ‘squared distance error’, respectively.

Since X is understood as a set rather than a single point, we define $|X|$ as the number of elements in the set X . The objective function O is nonnegative, continuous, and satisfies:

$$\lim_{\|W\| \rightarrow \infty} O(W) = \infty$$

uniformly in all directions in \mathbb{R}^2 or \mathbb{R}^3 . Therefore, by similar arguments as in [1, 2, 3], a solution X exists for the equation above.

Let $D_i, i = 1, \dots, I$ be the measurement closed ball centered at Z_i with radius d_i , and let S_i be its boundary, $D_i^o = D_i \setminus S_i$, and

$$S = \cup_{j=1}^I S_j.$$

In the following sections, we investigate the number of solutions and their locations when the number of measurements is one (Section 2), two (Section 3), and three (Section 4).

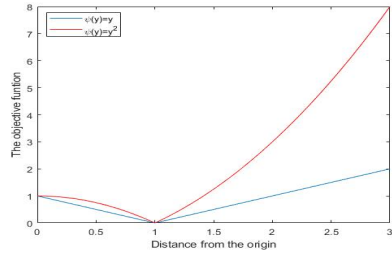
2 One measurement (I=1)

Let us first consider $I = 1$. The solution X is a circle in two dimensions and a sphere in three dimensions, both centered at \odot with a radius d_1 . In other words,

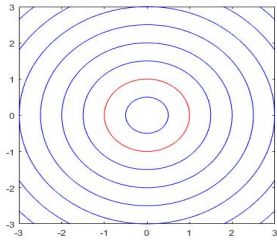
$$X = S_1, \text{ and } |X| = 1.$$

However, the behavior of the level set differs between the cases $\psi(y) = y$ and $\psi(y) = y^2$ as illustrated in Fig. 1. In the distance error case ($\psi(y) = y$), the Euclidean distance between the level sets remains uniform. In contrast, for the squared distance error case ($\psi(y) = y^2$), the Euclidean distance decreases as the location moves further away from the measurement circle (which is depicted as the unit circle in Fig. 1). Consequently, the minimization problem for squared distance error exhibits faster local convergence compared to the problem with distance error. This behavior is consistent in both two-dimensional and three-dimensional spaces.

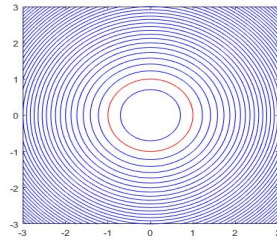
In figures 1 (g) and 1 (h), three dimensional gradient vectors are plotted. The gradient directions point outward if the starting points are outside the unit sphere (the 0-level set) and inward if the starting points are inside the unit sphere. The length of the gradient vectors remains constant in the distance error case in (g), whereas in the squared distance error case (h), the length is proportional to the distance between the starting point and the origin.



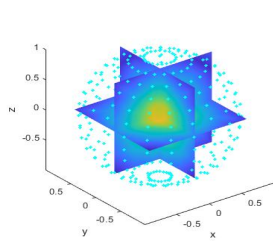
(a)



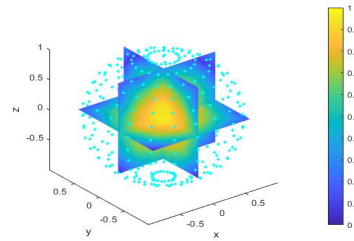
(b)



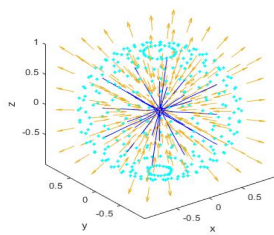
(c)



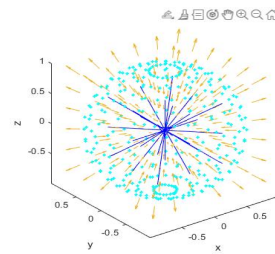
(d)



(e)



(f)



(g)

Figure 1: (a) The relation between the distance to Z_1 and the objective function is shown for both the distance error (blue line) and the squared distance error (red line). (b,c) The level sets of the objective function are depicted for $Z_1 = \mathbb{O}$ and $d_1 = 1$ in the xy -plane. The red line is the level set 0 and the blue lines are level sets for 0.5, 1, 1.5, and so on. A three dimensional sphere is plotted with blue dots. In (d) and (e), the values of level sets are displayed in xy -, yz -, zx - planes. In (f) and (g), the streamlines and the gradient vectors are shown. Specifically, (b),(d), and (e) corresponds to the distance error case, while (c),(d), and (g) represent the squared distance error case.

3 Two measurements (I=2)

Let us decompose $\mathbb{R}^n, n = 2, 3$ as four regions:

$$D_1 \setminus D_2, D_2 \setminus D_1, D_1 \cap D_2, (D_1 \cup D_2)^c.$$

Define $S_{12} = S_1 \cap S_2$ and $N_{\pm 1} = Z_1 \pm d_1 \frac{Z_2 - Z_1}{\|Z_2 - Z_1\|}$. Similarly, N_2, N_{-2} can be defined. If $S_{12} \neq \phi$, then $|S_{12}| = 1, 2$ for $n = 2$ and $|S_{12}| = 1, \infty$ for $n = 3$. Without loss of generality, assume $d_1 \geq d_2$.

The singular point for the objective function is denoted by Y_0 and its definition of Y_0 is different for distance and squared distance errors as follows:

$$Y_0 = \begin{cases} \frac{Z_1 + Z_2}{2} & \text{for } \psi(y) = y^2, \\ \overline{Z_1 Z_2} \setminus (D_1 \cup D_2) & \text{for } \psi(y) = y. \end{cases}$$

3.1 The squared distance error case ($\psi(y) = y^2$)

Note that $Y_0 = \frac{Z_1 + Z_2}{2}$ and $|Y_0| = 1$. We now state the following lemma:

Lemma 1. *Under the condition that the following sets are nonempty in $\mathbb{R}^n, n = 2, 3$, we have*

- (a) *The minimum in $(D_1 \cup D_2)^c$ is the point nearest to Y_0 .*
- (b) *The minimum in $D_1 \cap D_2$ is the farthest point to Y_0 .*
- (c) *The minimum in $D_1 \setminus D_2$ is N_1 if $N_1 \notin D_2$ and S_{12} if $N_1 \in D_2$.*

Proof. If $W \in (D_1 \cup D_2)^c$, then

$$O(W) = \|W - Z_1\|^2 + \|W - Z_2\|^2 - d_1^2 - d_2^2 = 2\|W - Y_0\|^2 + \text{Constant}.$$

Thus, we (a) is proven.

If $W \in D_1 \cap D_2$, then

$$O(W) = -\|W - Z_1\|^2 - \|W - Z_2\|^2 + d_1^2 + d_2^2 = -2\|W - Y_0\|^2 + \text{Constant}.$$

Thus, (b) is proven.

If $W \in D_1 \setminus D_2$, then

$$O(W) = (Z_1 - Z_2) \cdot W + \text{Constant}.$$

Thus, (c) is proven. □

Based on this lemma, we present the following theorem:

Theorem 2. *In the case of two measurements with $\psi(y) = y^2$ and $n = 2, 3$, the followings minimums occur:*

- (a) *If $d_1 \leq \frac{\|Z_2 - Z_1\|}{2}$, then $X = Y_0$.*
- (b) *If $\frac{\|Z_2 - Z_1\|}{2} \leq d_1 < \|Z_2 - Z_1\|$ and $d_1 + d_2 \leq \|Z_2 - Z_1\|$, then $X = N_1$.*
- (c) *If $d_1 - d_2 < \|Z_2 - Z_1\| < d_1 + d_2$, then $X = S_{12}$.*
- (d) *If $d_1 - d_2 \geq \|Z_2 - Z_1\|$, then $X = N_1$.*

Corollary 3. *In the two-dimensional case, the number of solutions is either 1 or 2:*

$$\begin{cases} |X| = 1 & \text{if and only if } \|Z_2 - Z_1\| \geq d_1 + d_2 \text{ or } \|Z_2 - Z_1\| \leq d_1 - d_2, \\ |X| = 2 & \text{if and only if } d_1 - d_2 < \|Z_2 - Z_1\| < d_1 + d_2. \end{cases}$$

Corollary 4. *In the three-dimensional case, the number of solutions is either 1 or ∞ :*

$$\begin{cases} |X| = 1 & \text{if and only if } \|Z_2 - Z_1\| \geq d_1 + d_2 \text{ or } \|Z_2 - Z_1\| \leq d_1 - d_2, \\ |X| = \infty & \text{if and only if } d_1 - d_2 < \|Z_2 - Z_1\| < d_1 + d_2. \end{cases}$$

3.2 The distance error case ($\psi(y) = y$)

Note that $Y_0 = \overline{Z_1 Z_2} \setminus (D_1 \cup D_2)$ and $|Y_0| = 0, 1, \infty$.

Lemma 5. *Under the condition that the following sets are nonempty in $\mathbb{R}^n, n = 2, 3$, we have*

(a) *The minimum in $(D_1 \cup D_2)^c$ is the nearest point to $\overline{Z_1 Z_2}$ as follows :*

$$\begin{cases} Y_0 & \text{if } d_1 + d_2 \leq \|Z_1 - Z_2\|, \\ S_{12} & \text{if } d_1 - d_2 < \|Z_1 - Z_2\| < d_1 + d_2, \\ N_1 & \text{if } d_1 - d_2 \geq \|Z_1 - Z_2\|. \end{cases}$$

(b) *The minimum in $D_1 \cap D_2$ is the farest point from $\overline{Z_1 Z_2}$ as follows:*

$$\begin{cases} S_{12} & \text{if } d_1 - d_2 < \|Z_1 - Z_2\| < d_1 + d_2, \\ N_{-2} & \text{if } d_1 - d_2 \geq \|Z_1 - Z_2\|. \end{cases}$$

(c) *The minimum in $D_1 \setminus D_2$ is as follows:*

$$\begin{cases} N_1 & \text{if } d_1 + d_2 \leq \|Z_1 - Z_2\|, \\ S_{12} & \text{if } d_1 - d_2 < \|Z_1 - Z_2\| < d_1 + d_2, \\ \overline{N_{-2} N_1} & \text{if } d_1 - d_2 \geq \|Z_1 - Z_2\|. \end{cases}$$

Proof. If $W \in (D_1 \cup D_2)^c$, we have

$$O(W) = \|W - Z_1\| + \|W - Z_2\| - d_1 - d_2.$$

Thus, (a) is proven.

If $W \in D_1 \cap D_2$, we have

$$O(W) = -\|W - Z_1\| - \|W - Z_2\| + d_1 + d_2.$$

Thus, (b) is proven.

If $W \in D_1 \setminus D_2$, we have

$$O(W) = \|W - Z_2\| - \|W - Z_1\| + d_1 - d_2.$$

Thus, (c) is proven. □

Based on this lemma, we can state the following theorem:

Theorem 6. *For two measurements and distance error minimization with $n = 2, 3$, the followings minimums occur:*

(a) *If $d_1 + d_2 \leq \|Z_2 - Z_1\|$, then $X = Y_0$.*

(b) *If $d_1 - d_2 \leq \|Z_2 - Z_1\| \leq d_1 + d_2$, then $X = S_{12}$.*

(c) *If $d_1 - d_2 \geq \|Z_2 - Z_1\|$, then $X = \overline{N_{-2} N_1}$.*

Corollary 7. *In the two-dimensional case, the number of solutions can be 1, 2, or ∞ :*

$$\begin{cases} |X| = 1 & \text{if and only if } \|Z_2 - Z_1\| = d_1 + d_2 \text{ or } d_1 - d_2, \\ |X| = 2 & \text{if and only if } d_1 - d_2 < \|Z_2 - Z_1\| < d_1 + d_2, \\ |X| = \infty & \text{if and only if } \|Z_2 - Z_1\| > d_1 + d_2 \text{ or } \|Z_2 - Z_1\| < d_1 - d_2. \end{cases}$$

Corollary 8. *In the three-dimensional case, the number of solutions can be 1 or ∞ :*

$$\begin{cases} |X| = 1 & \text{if and only if } \|Z_2 - Z_1\| = d_1 + d_2 \text{ or } d_1 - d_2, \\ |X| = \infty & \text{if and only if } \|Z_2 - Z_1\| \neq d_1 + d_2 \text{ and } d_1 - d_2. \end{cases}$$

Case	$\psi(y) = y$ Solution X	$\psi(y) = y$ X : 2D	$\psi(y) = y$ X :3D	$\psi(y) = y^2$ Solution X	$\psi(y) = y^2$ X : 2D	$\psi(y) = y^2$ X :3D
$d_1 < \frac{\ Z_1 Z_2\ }{2}$	Y_0	∞	∞	Y_0	1	1
$\frac{\ Z_1 Z_2\ }{2} \leq d_1 < \ Z_1 Z_2\ $, $d_1 + d_2 \leq \ Z_1 Z_2\ $	Y_0	∞ (*1)	∞ (*1)	N_1	1	1
$d_1 - d_2 < \ Z_1 Z_2\ < d_1 + d_2$	S_{12}	2	∞	S_{12}	2	∞
$d_1 - d_2 \geq \ Z_1 Z_2\ $	$N_{-2} N_1$	∞ (*1)	∞ (*1)	N_1	1	1

Table 1: The solution location and numbers in 2 measurements.

*1: The number of X is 1 only for the case $\|Z_1 Z_2\| = d_1 + d_2$ or $d_1 - d_2$.

Case	$\psi(y) = y$ X : 2D	$\psi(y) = y$ X :3D	$\psi(y) = y^2$ X : 2D	$\psi(y) = y^2$ X :3D
$d_1 < \frac{\ Z_1 Z_2\ }{2}$	Fig.2(a)	Fig.3(a)	Fig.2(b)	Fig.3(b)
$\frac{\ Z_1 Z_2\ }{2} \leq d_1 < \ Z_1 Z_2\ $, $d_1 + d_2 \leq \ Z_1 Z_2\ $	Fig.2(c)	Fig.3(c)	Fig.2(d)	Fig.3(d)
$d_1 - d_2 < \ Z_1 Z_2\ < d_1 + d_2$	Fig.2(e)	Fig.3(e)	Fig.2(f)	Fig.3(f)
$d_1 - d_2 \geq \ Z_1 Z_2\ $	Fig.2(g)	Fig.3(g)	Fig.2(h)	Fig.3(h)

Table 2: The figures in Fig. 2 and Fig. 3 corresponding to each cases in Table 1

3.3 The comparison

Summarizing the results in Subsection 3.1 and 3.2, the outcomes are compiled in Table 1. The corresponding figures for each case listed in Table 1 are displayed in Fig. 2 and Fig. 3, representing the two- and three-dimensional cases, respectively. The correspondence between these figures and the cases in Table 1 is outlined in Table 2. It can be observed that the numerical results shown in the figures align with the theoretical results in the aforementioned subsections.

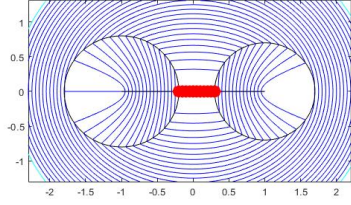
In Fig.2, which depicts the two dimensional case, the level sets of the objective functions are visualized using the ‘contour’ function in Matlab. Here, the minimum value of the objective function is denoted by m . The blue contours represent level sets ranging from m to $m + 3$ with an interval of 0.1, while the cyan countours depict level sets from $m + 3$ to $m + 50$ with an interval of 1. The red markers indicate the theoretical minimum points for each case. For the squared distance case shown in Fig. 2 (b),(d),(f), and (h), the level sets are vertically confined within two disks that do not intersect with the other disk. In contrast, for the distance error case, illustrated in Fig. 2 (a),(c), and (g), the level sets are more horizontally oriented near the solutions.

The three dimensional results are presented in Fig. fig:Meas2Dim3 under similar conditions on Z_1, Z_2, d_1 and d_2 . Two spheres are depicted with black and green dots, while the level sets shown on the planes $x = -1, x = 1, y = 0.1$, and $z = -0.1$. The gradient directions on grid points, with a step size of 0.5 in all three axis directions, are illustrated using Matlab’s ‘quiver’ command. Streamlines are also plotted in these figures. In the squared distance error cases (Fig. 3 (b),(d),(f), and (g)), the streamlines inside two balls that are not contained within the other ball run parallel to the x -axis, where the centers of the two balls lie. On the other hand, in the distance error cases (Fig. 3 (a), (c), (e), and (f)), the streamlines inside the black ball, which is not contained within the green ball, converges toward the negative x -axis direction.

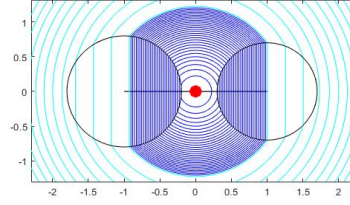
4 Three measurements (I=3)

Let $1A = A$ and $0A = \phi$ for any set A . Define

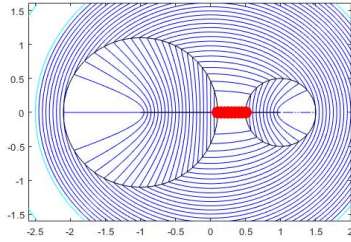
$$R_{ijk} = \overline{(iD_1 \cup (1-i)D_1^c) \cap (jD_2 \cup (1-j)D_2^c) \cap (kD_3 \cup (1-k)D_3^c)},$$



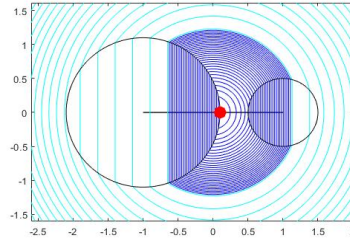
(a)



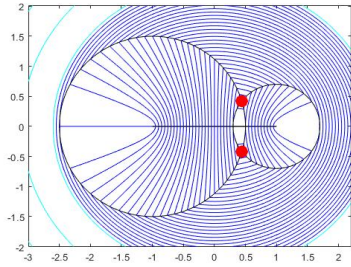
(b)



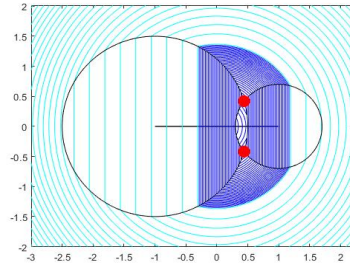
(c)



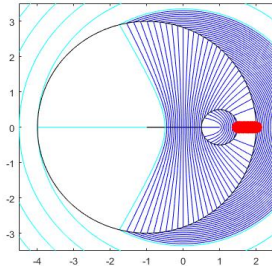
(d)



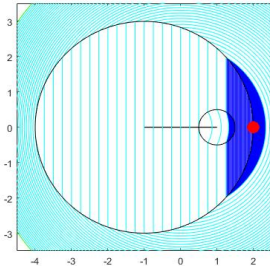
(e)



(f)



(g)



(h)

Figure 2: The location of the two-dimensional sources for (a,c,e,g) $\psi(y) = y$ and (b,d,f,h) $\psi(y) = y^2$ when (a,b) $d_1 \leq \frac{\|Z_1 Z_2\|}{2}$ (c,d) $\frac{\|Z_1 Z_2\|}{2} \leq d_1 < \|Z_1 Z_2\|$ and $d_1 + d_2 \leq \|Z_1 Z_2\|$ (e,f) $d_1 - d_2 < \|Z_1 Z_2\| < d_1 + d_2$ (g,h) $d_1 - d_2 \geq \|Z_1 Z_2\|$

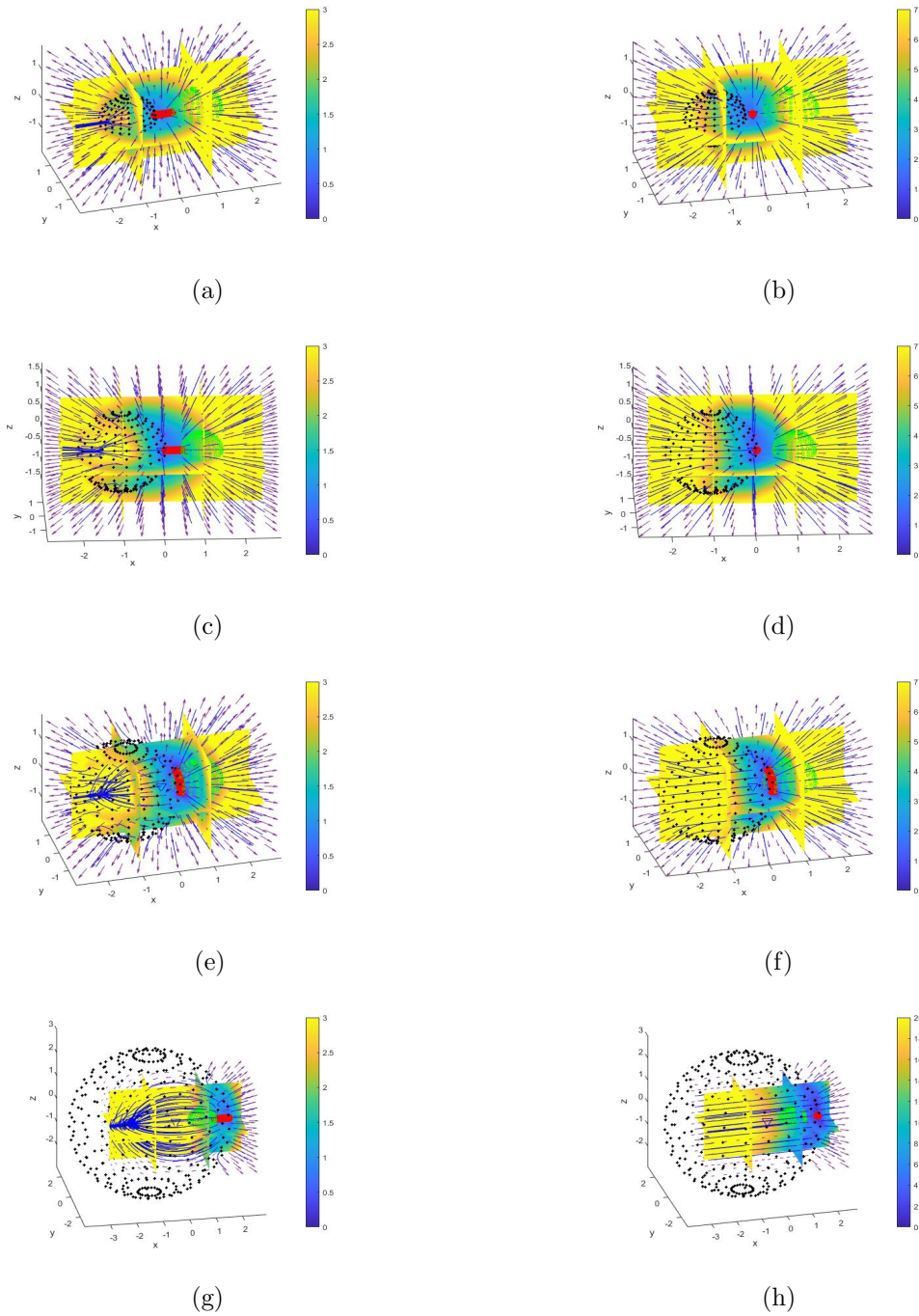


Figure 3: The location of the three-dimensional sources for (a,c,e,g) $\psi(y) = y$ and (b,d,f,h) $\psi(y) = y^2$ when (a,b) $d_1 \leq \frac{\|Z_1 Z_2\|}{2}$ (c,d) $\frac{\|Z_1 Z_2\|}{2} \leq d_1 < \|Z_1 Z_2\|$ and $d_1 + d_2 \leq \|Z_1 Z_2\|$ (e,f) $d_1 - d_2 < \|Z_1 Z_2\| < d_1 + d_2$ (g,h) $d_1 - d_2 \geq \|Z_1 Z_2\|$.

for $i, j, k \in \{0, 1\}$. Also, define $R_l = \cup_{i+j+k=l} R_{ijk}$.

Let Δ denote the measurement triangle $\Delta Z_1 Z_2 Z_3$, α be the plane containing Δ , and $K = \Delta \cap R_0 \cap \alpha$.

The critical points of the objective function O can be classified as Y_{ijk} where $i, j, k \in \{0, 1\}$ and $Y_{ijk} \subset R_{ijk}$. Among these, only Y_0, Y_{100}, Y_{010} , and Y_{001} can be local minima, while the others may be local maxima. Therefore,

$$Y = \{Y_0 \cap R_0, Y_{100} \cap R_{100}, Y_{010} \cap R_{010}, Y_{001} \cap R_{001}\},$$

is the set containing local minima and critical points. Let us define them for the cases $\psi(y) = y^2$ and $\psi(y) = y$.

For the squared distance case $\psi(y) = y^2$, the critical points are defined as:

$$\begin{aligned} Y_0 &= \frac{Z_1 + Z_2 + Z_3}{3}, \\ Y_{100} &= -Z_1 + Z_2 + Z_3, \\ Y_{010} &= Z_1 - Z_2 + Z_3, \\ Y_{001} &= Z_1 + Z_2 - Z_3. \end{aligned}$$

If $Y_0 \in R_0, Y_{100} \in R_{100}, Y_{010} \in R_{010}$, or $Y_{001} \in R_{001}$, then these points are critical points for the objective function O . It is proven in [2] that $|\{Y_0 \cap R_0, Y_{100} \cap R_{100}, Y_{010} \cap R_{010}, Y_{001} \cap R_{001}\}| \leq 1$, meaning that the set contains either 0 or 1 point.

For the distance error case $\psi(y) = y$, Y_0 is defined as the Fermat point of the triangle $\Delta Z_1 Z_2 Z_3$. To describe Y_{100} , consider the plane α containing Z_1, Z_2 , and Z_3 . In this plane, two half planes are divided by the line $\overleftrightarrow{Z_2 Z_3}$. Consider a point \tilde{Z}_1 in the half plane containing Z_1 such that $\tilde{Z}_1 Z_2 Z_3$ is an equilateral triangle. Let C be the circumscribed circle of $\Delta \tilde{Z}_1 Z_2 Z_3$ and \tilde{C} be the arc of C that lies in the other half-plane and connects Z_2 and Z_3 . Y_{100} is defined as the intersection of the line $\tilde{Z}_1 Z_1$ and \tilde{C} , which can either be empty or consist of a single one point if $\tilde{Z}_1 \neq Z_1$, or be the entire arc if $\tilde{Z}_1 = Z_1$. Similarly, Y_{010} and Y_{001} are defined.

If $\Delta Z_1 Z_2 Z_3$ is not equilateral, $|Y|$ equals 0 or 1, and if $\Delta Z_1 Z_2 Z_3$ is equilateral, $|Y| = \infty$.

Let

$$S_{123} = S_1 \cap S_2 \cap S_3,$$

and

$$S_{ij} = S_i \cap S_j,$$

for $i, j \in \{1, 2, 3\}$.

For both cases of ψ , Y_0 lies in $\overline{\Delta}$. Define S_{12}^+ and S_{12}^- as the points in S_{12} which are closest to and farthest from Y_0 , respectively. Note that S_{12}^+ and S_{12}^- lie in *alpha*. Similarly, S_{23}^{\pm} and S_{31}^{\pm} are defined.

The definitions of N_i , for $i = 1, 2, 3$, as members of S_i , vary depending on ψ and will be explained in the following subsections.

The results in this section are derived from the papers [2, 3] for $\psi(y) = y^2$ and the paper [1] for $\psi(y) = y$ in two-dimensional case. The following two lemmas illustrate the difference between the two- and three-dimensional cases:

Lemma 9. *In the two dimensional case with $n = 2$, the following hold:*

- If Z_1, Z_2 , and Z_3 are not collinear, $|S_{123}| = 0$, or 1.
- If $|S_{123}| = 1$, then $X = S_{123}$.
- If R_{100} is nonempty, then it is either connected or has two connected components.
- If all of R_{100}, R_{010} , and R_{001} are nonempty, then $|S_{123}| = 0$.

The proof is straightforward and can be found in [1, 2, 3]. However, in the three-dimensional case, the situation differs significantly from the two-dimensional case, as described below:

Lemma 10. *In the three dimensional case with $n = 3$, the following hold:*

- If Z_1, Z_2, Z_3 does not lies on the same line, $|S_{123}| = 0, 1$, or 2 .
- If $|S_{123}| = 1$ or 2 , then $X = S_{123}$.
- If R_{100} is nonempty, then it is connected.
- If all of $R_{100}, R_{010}, R_{001}$ are nonempty, then $|S_{123}| = 2$.

Proof. S_{12} can be empty or one point or a circle. S_{123} could be empty, a single point, or two points. If $S_{123} \neq \phi$, then $O(S_{123}) = 0$ and $X = S_{123}$.

Assume R_{100} is nonempty. Then, one of two points $Z_1 - d_1 \frac{Z_2 - Z_1}{\|Z_2 - Z_1\|}$ or $Z_1 - d_1 \frac{Z_3 - Z_1}{\|Z_3 - Z_1\|}$, which are the farrest points from Z_2 and Z_3 respectively, is contained in R_{100} . Therefore, $R_{100} \cap \alpha$ is also nonempty.

If $D_2 \cap D_3 = \phi, D_2 \subset D_3$, or $D_3 \subset D_2$, then R_{100} is easily proven to be connected. Otherwise, we have $|d_2 - d_3| \leq \|Z_2 Z_3\| \leq d_2 + d_3$. Let the plane passing through Z_1, Z_2 , and Z_3 be denoted as α . Since the region R_{100} is symmetric with respect to the plane α , we only need to consider the half-space divided by α . Let β be the plane containing S_{23} and orthogonal to α . Let B be the foot of the perpendicular from Z_1 to the plane β . Then, $D_1 \cap \beta$ is the disk centered at B with radius $\sqrt{d_1^2 - \|Z_1 B\|^2}$ and this disk contains S_{23} . Hence, in this case also, R_{100} is also connected. Thus, in all the cases, if R_{100} is nonempty, it is connected.

If all of $R_{100}, R_{010}, R_{001}$ are nonempty, then $R_{100} \cap \alpha, R_{010} \cap \alpha, R_{001} \cap \alpha$ are all nonempty, as shown previously. $R_3 \cap \alpha$ forms a spherical triangle in α . Let α^k be the hyperplane parallel to α at a distance k , and let Z_1^k, Z_2^k, Z_3^k be the intersection points between α^k and the perpendicular to α passing through Z_1, Z_2, Z_3 , respectively. The radius of a circle in the plane α^k centered at Z_j^k (for $j = 1, 2, 3$) becomes $\sqrt{\max(d_j^2 - k^2, 0)}$. Therefore, there exists a number $k > 0$ such that $R_3 \cap \alpha_k$ is a singel point. By symmetry with respect to the plane α , there are two points such the line joining them is orthogonal to α . These two points must be S_{123} . \square

4.1 The squared distance error case ($\psi(y) = y^2$)

By Lemma 9 and Lemma 10, if $S_{123} \neq \phi$, then $X = S_{123}$. Form now on, consider the nontrivial case where $S_{123} = \phi$. The results vary depending on whether the dimension is $n = 2$ or $n = 3$.

In two dimension, the following cases arise:

1. $R_3 = \phi$
2. $R_3 \neq \phi$ and one of $R_{100}, R_{010}, R_{001}$ is empty.
3. $R_3 \neq \phi$ and one of $R_{100}, R_{010}, R_{001}$ is nonempty but disconnected.
4. $R_3 \neq \phi$ and all of $R_{100}, R_{010}, R_{001}$ are nonempty and connected.

In three dimensions, with the aid of Lemma 10, we enounter the following simple cases:

1. $R_3 = \phi$
2. $R_3 \neq \phi$ and one of $R_{100}, R_{010}, R_{001}$ is empty.

In the two-dimensional case 3, $X = X_{100}$ and $|X| = 1$ [2]. In case 4, $X \subset \{S_{12}^\pm, S_{23}^\pm, S_{31}^\pm\}$ and $|X| \leq 5$ [3]. In this subsection, focus is placed on cases 1 and 2 in both two or three dimensions, which covers all the possible scenarios in three dimensions. In case 2, assume without loss of generality that $R_{001} = \phi$, which means $D_3 \subset D_1 \cup D_2$. Therefore, the analysis in this subsection is restricted to the cases where $R_3 = \phi$ or $D_3 \subset D_1 \cup D_2$. Define

$$N_{ij} = Z_i + d_i \frac{Y_j - Z_i}{\|Y_j - Z_i\|}, \quad N_i := N_{ii}, \quad i, j \in \{1, 2, 3\}.$$

Following [2], the following results hold in both two and three dimensions:

- If $D_3 \subset D_1 \cap D_2$ and $S_{12} \neq \phi$, then $X = S_{12}^+$.
- If $D_3 \subset D_1$ and $D_2 \subset D_1$, then $X = X_{100}$, meaning

$$\begin{cases} X = Y_{100} & \text{if } Y_{100} \in R_{100}, \\ X = N_1 & \text{if } Y_{100} \notin D_1, \\ X = N_{21} & \text{if } Y_{100} \in D_2, N_{21} \in R_{100}, \\ X = S_{23}^+ & \text{if } Y_{100} \in D_2, N_{21} \in D_2. \end{cases}$$

- If K is nonempty, then $R_3 = \phi$ and $X = X_0$, meaning,

$$\begin{cases} X = Y_0 & \text{if } Y_0 \in R_0, \\ X = N_1 & \text{if } Y_0 \in D_1, N_1 \in R_0, \\ X = S_{12}^+ & \text{if } Y_0 \in D_1, N_1 \in D_2. \end{cases}$$

- If $K = \phi$ and $R_3 = \phi$, then there exists a ball(3D) or a disk(2D) that intersects the other two balls or two disks. Let this ball or disk be D_1 . Then, we have $X = X_{100}$, meaning:

$$\begin{cases} X = Y_{100} & \text{if } Y_{100} \in R_{100}, \\ X = N_1 & \text{if } Y_{100}, N_1 \in R_0, \\ X = N_{21} & \text{if } Y_{100} \in D_2, N_{21} \in R_{100}, \\ X = S_{12}^+ & \text{if } Y_{100} \in R_0, N_1 \in D_2 \text{ or } Y_{100} \in D_2, N_{21} \in R_0. \end{cases}$$

Corollary 11. *In two dimensional case with $n = 2$, the number of solutions can be 1, 2, 3, 4, or 5:*

$$\begin{cases} |X| \leq 5, & X \subset \{S_{12}^\pm, S_{23}^\pm, S_{31}^\pm\} \\ & \text{if } |S_{123}| = 0, R_3 \neq \phi, \text{ and all of } R_{100}, R_{010}, R_{001} \text{ are nonempty and connected,} \\ |X| = 1 & \text{Otherwise.} \end{cases}$$

Corollary 12. *In three dimensional case with $n = 3$, the number of solutions can be 1 or 2:*

$$\begin{cases} |X| = 1 & \text{if } |S_{123}| = 0, 1, \\ |X| = 2 & \text{if } |S_{123}| = 2. \end{cases}$$

Suppose that $\|Z_1 Z_3\| = \|Z_2 Z_3\|$, $d_1 = d_2$, and $d_3^2 = d_1^2 - \|Z_1 Z_3\|^2$, and define

$$P = \frac{\|Z_1 Z_2\|^2}{4} + \left(\|Z_1 Z_3\|^2 - \frac{\|Z_1 Z_2\|^2}{4} \right) \left(\frac{\|Z_1 Z_3\|^2 + \|Z_1 Z_2\|^2}{\|Z_1 Z_3\|^2 - \|Z_1 Z_2\|^2} \right)^2.$$

We also have the following detailed interesting non-uniqueness results in the two dimensional case [3]:

$$\begin{cases} |X| = 5, X = \{S_{12}^+, S_{23}^\pm, S_{31}^\pm\} & \text{if } \|Z_1 Z_3\| > \|Z_1 Z_2\| \text{ and } d_1^2 = P. \\ |X| = 4, X = \{S_{23}^\pm, S_{31}^\pm\} & \text{if } \|Z_1 Z_3\| > \|Z_1 Z_2\| \text{ and } d_1^2 > P. \\ |X| = 1, X = S_{12}^+ & \text{if } \|Z_1 Z_3\| \leq \|Z_1 Z_2\| \text{ or } d_1^2 \leq P. \end{cases}$$

Futhermore, the first condition is both sufficient and necessary for $|X| = 5$, with reordering if needed. Specifically,

$$|X| = 5 \text{ if and only if } \|Z_1 Z_3\| = \|Z_2 Z_3\| > \|Z_1 Z_2\|, d_3^2 = d_1^2 - \|Z_1 Z_3\|^2, \text{ and } d_1^2 = P,$$

where reordering may be required. In this scenario, X is given by $X = X = \{S_{12}^+, S_{23}^\pm, S_{31}^\pm\}$, again with reordering if necessary.

	$\psi(y) = y$ [1]	$\psi(y) = y^2$ [2]
$S_{123} \neq \phi$	$X = S_{123}$ (Fig.4(a))	$X = S_{123}$ (Fig.4(b))
$Y_0 \in R_0$	$X = Y_0$ (Fig.4(c))	$X = Y_0$ (Fig.4(d))
$Y_0 \in R_{010}, T = \phi, K \neq \phi, N_2 \in R_0$	$X = N_2$ (Fig.4(e))	$X = N_2$ (Fig.4(f))
$Y_{100} \cap R_{100} \neq \phi$ and Δ is equilateral	$X = Y_{100} \cap R_{100}, X = \infty$ (Fig.4(g))	$X = Y_{010}, X = 1$ (Fig.4(h))
$ T = 2$	$X = T$ (Fig.5(a))	$X = N_1$ (Fig.5(b))
$ T = 1, N_1 \in D_2$	$X = T \cap R_0$ (Fig.5(c))	$X = S_{12}^+$ (Fig.5(d))

Table 3: Comparison for the solutions for $\psi(y)$ and $\psi(y) = y^2$ in two dimensions.

The exact location of the solution X is not precisely determined in the two dimensional case when

$$|S_{123}| = 0 \text{ and } R_3 \neq \phi \text{ and all of } R_{100}, R_{010}, R_{001} \text{ are nonempty and connected.}$$

In this case, it is only known that $X \subset \{S_{12}^\pm, S_{23}^\pm, S_{31}^\pm\}$. However, in the isocetes measurement cases, where $\|Z_1 Z_3\| = \|Z_2 Z_3\|$ and $d_1 = d_2$, the exact location and the number of the solution are known [3].

4.2 The distance error case ($\psi(y) = y$)

By Lemma 9 and Lemma 10, if $S_{123} \neq \phi$, then $X = S_{123}$. Now, consider only the case when $S_{123} = \phi$. Define $K = R_0 \cap \Delta$ and

$$T = \alpha \cap (S_1 \cap \overline{Z_2 Z_3} \cap \partial R_{100}) \cup (S_2 \cap \overline{Z_1 Z_3} \cap \partial R_{010}) \cup (S_3 \cap \overline{Z_1 Z_2} \cap \partial R_{001}).$$

Note that $T \neq \phi$, then $K \neq \phi$. Next, let N_1 be defined as the point on S_1 where the sum of distances to Z_2 and Z_3 is minimized. The point is uniquely defined if $S_1 \cap \overline{Z_2 Z_3} = \phi$, but there may be two such points, otherwise.

The number and location of solutions, whether in two or three dimensions, can be summarized as follows (the proof for the two dimensional case is provided in [1]):

$$\left\{ \begin{array}{ll} X = S_{123} & \text{if } S_{123} \neq \phi, \\ X = Y_0 & \text{if } Y_0 \in R_0, \\ X = Y_{100} & \text{if } Y_{100} \in R_{100}, \\ X = T \text{ and } |X| = 1 \text{ or } 2 & \text{if } T \neq \phi, \\ X = N_1 & \text{if } T = \phi, K \neq \phi, Y_0 \in R_{100}, N_1 \in R_0 \\ X = S_{12}^+ & \text{if } (T = \phi, K \neq \phi, Y_0 \in R_{110}) \text{ or } (T = \phi, K \neq \phi, Y_0 \in R_{100}, N_1 \in D_2) \\ X = \tilde{C} \cap R_{100} \text{ and } |X| = \infty & \text{if } \Delta \text{ is equilateral and } \frac{\sqrt{3}}{2}d_1 > \|Z_1 - Z_2\| > d_2 + d_3. \end{array} \right.$$

These cases do not cover all possible scenarios, but they do address all situations where $K \neq \phi$. For the case where $K = \phi$, much remains unknown.

4.3 The comparison

In the two dimensional case, we compared the solutions for the distance error ($\psi(y) = y$) and squared distance error ($\psi(y) = y^2$) cases, as illustrated in Figures 4 and 5. The detailed settings for the measurement triangle, the measurement data, and corresponding solutions in the figures are explained in Table 3.

It is important to note that the definitions of Y_0, N_2 , and Y_{100} vary depending on the choice of ψ . For instance, Y_0 is referred as the ‘Fermat point’ for $\psi(y) = y$ and as the ‘center of gravity’ for $\psi(y) = y^2$. Additionally, in the case of an equilateral measurement triangle, $|Y_{100}|$ is ∞ for $\psi(y) = y$ and 1 for $\psi(y) = y^2$.

In Figures 4, 5, and 6, which depicts the two dimensional case and three measurements, the level sets of the objective functions are visualized using the ‘contour’ function in Matlab. Here, the minimum value of the objective function is denoted by m .

	$\psi(y) = y$	$\psi(y) = y^2$
$S_{123} \neq \phi$	$X = S_{123}$ (Fig.7(a))	$X = S_{123}$ (Fig.7(b))
$ T = 2$	$X = T$ (Fig.7(c))	$X = N_1$ (Fig.7(d))
$ T = 1, N_1 \in D_2$	$X = T \cap R_0$ (Fig.7(e))	$X = S_{12}^+$ (Fig.7(f))
$Y_{100} \cap R_{100} \neq \phi$ and Δ is equilateral	$X = Y_{100} \cap R_{100}, X = \infty$ (Fig.7(g))	$X = Y_{010}, X = 1$ (Fig.7(h))

Table 4: Comparison for the solutions for $\psi(y)$ and $\psi(y) = y^2$ in three dimensions.

- The blue contours represent level sets ranging from m to $m + 3$ with an interval of 0.5,
- The cyan countours represent level sets from $m + 3$ to $m + 50$ with an interval of 2.
- The green countours represent level sets from $m + 50$ to $m + 200$ with an interval of 10.

The red markers indicate the theoretical minimum points for each case.

The level sets for the distance case shown in Fig. 4 (a),(c),(e),(g), Fig. 5 (a) and (c), are more dependent on the vertices Z_1, Z_2 , and Z_3 compared to the level sets for the squared distance error case, shown in Fig. 4 (b),(d),(f),(h), Fig. 5 (b) and (d),

The location of sources when $K = \phi$ is only known for $\psi(y) = y^2$. In Fig. 6, we illustrate the case when $|X| = 2, 3, 4, 5$ for flat, sharp isoscles and equilateral triangles. For detailed explanations of these cases, refer to [3] As shown in Corollary 12, it is important to note that the number of solutions for $\psi(y) = y^2$ and three dimensional case, is less than 2.

The number of solutions in two-dimensional cases with squared distance error can be 2, 3, 4, or 5 . As proved in [3], the maximum number of solutions is 5. Examples illustrating these cases are provided in Fig. 6.

In the three dimensional case, we compared the solutions for the distance error ($\psi(y) = y$) and squared distance error ($\psi(y) = y^2$) scenarios, as illustrated in Fig. 7. Detailed settings for the measurement triangle, the measurement data, and corresponding solutions are provided in Table 4.

Three spheres are depicted with blue, green, and cyan dots. The gradient directions on grid points, with a step size of 1.5 in all three axis directions, are illustrated using Matlab's 'quiver' command. Streamlines are also plotted in these figures.

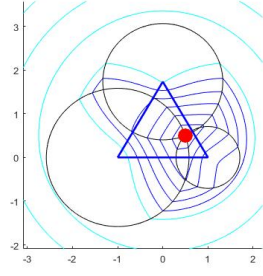
5 Conclusion

In this study, we addressed the source localization problem by fomulating two primary minimization problems: distance error and squared distance error minimization. We investigated these problems in both three-dimensional space,which is the standard scenario, and in two-dimensional space as a simplified case. Additionally, we analyzed the number of possible source solutions when the number of measurements is fewer than three.

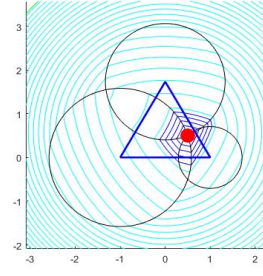
Even though a single measurement yields a solution ththat is a disk in 2D and a ball in 3D for both minimizations, the step lengths of the level sets for the distance error cases are more uniform compared to the squared distance error cases.

For two measruements, most senarios for the distance error case produced an infinite number of solutions, even in two dimensions. However, in the two-dimensional squared distance error case, the maximum number of solutions is 2, while in three-dimensional squared distance error case, an infinite number of solutions occur s in only one of four cases. This resultt is related to the fact that the intersection of two disks is two-point set in two dimension, whereas the intersection of two balls is a circle with infinite points in three dimension, provided the interesection is nonempty nor one-point set and neither ball or disk does not contain the other..

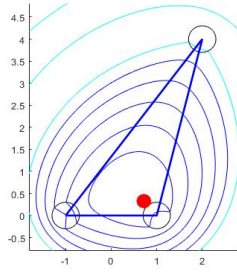
The scenarios for three measurements are not fully explored. The maximum number of solutions is infinite for the distance error case, 5 for two-dimensional squared distance case, and 2 for three dimensional squared



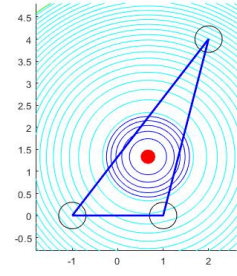
(a)



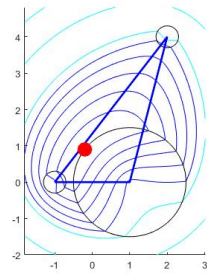
(b)



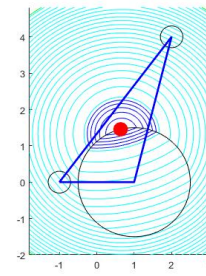
(c)



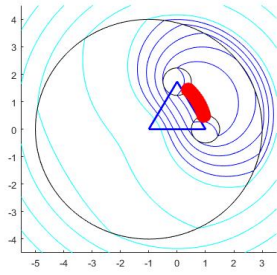
(d)



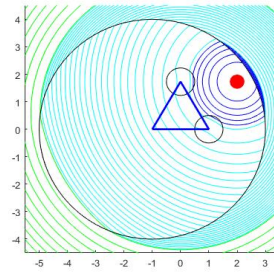
(e)



(f)



(g)



(h)

Figure 4: The source locations for cases (a,c,e,g) are based on $\psi(y) = y$, while those for cases (b,d,f,h) are based on $\psi(y) = y^2$. The conditions for each case are (a,b) $d_1 \leq \frac{\|Z_1 Z_2\|}{2}$ (c,d) $\frac{\|Z_1 Z_2\|}{2} \leq d_1 < \|Z_1 Z_2\|$, $d_1 + d_2 \leq \|Z_1 Z_2\|$ (e,f) $d_1 - d_2 < \|Z_1 Z_2\| < d_1 + d_2$ (g,h) $d_1 - d_2 \geq \|Z_1 Z_2\|$. For detailed description of these cases see Tab. 3.

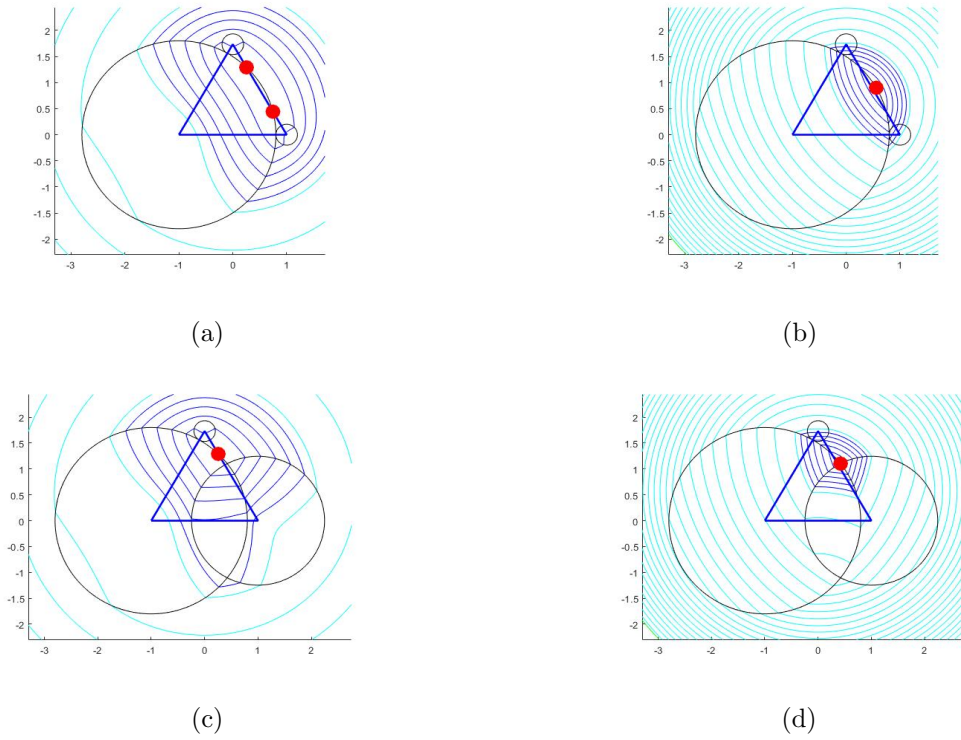
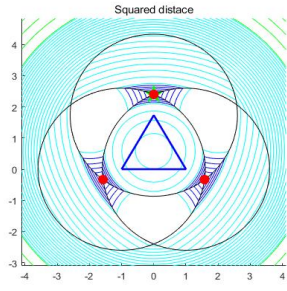
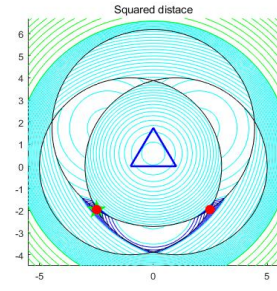


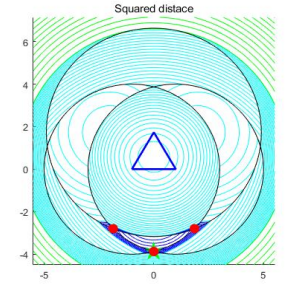
Figure 5: The source locations for cases (a,c,e,g) are based on $\psi(y) = y$, while those for cases (b,d,f,h) are based on $\psi(y) = y^2$. The conditions for each case are (a,b) $|T| = 2$ and (c,d) $|T| = 1, N_1 \in D_2$. For detailed description of these cases see Tab. 3.



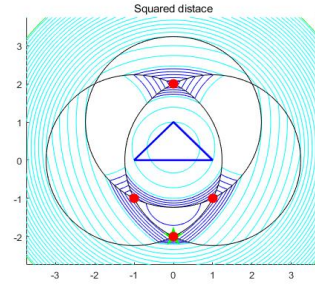
(a)



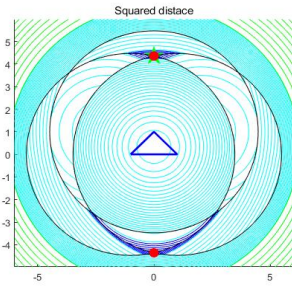
(b)



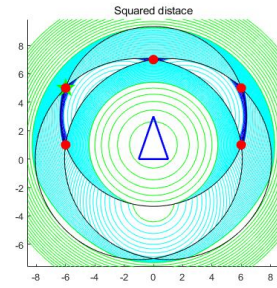
(c)



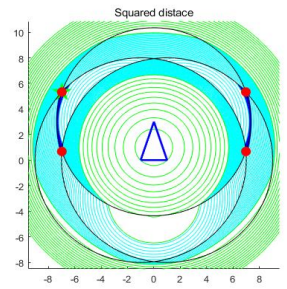
(d)



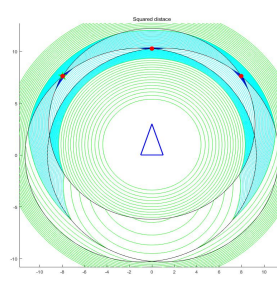
(e)



(f)



(g)



(h)

Figure 6: The location of the sources for $\psi(y) = y^2$ with $d_1 = d_2$ are as follows: For the equilateral triangle cases: (a,c) 3 solutions (b) 4 solutions. For flat isosceles cases: (d) 4 solutions (e) 2 solutions. For sharp isosceles cases: (f) 5 solutions (g) 4 solutions (h) 3 solutions.

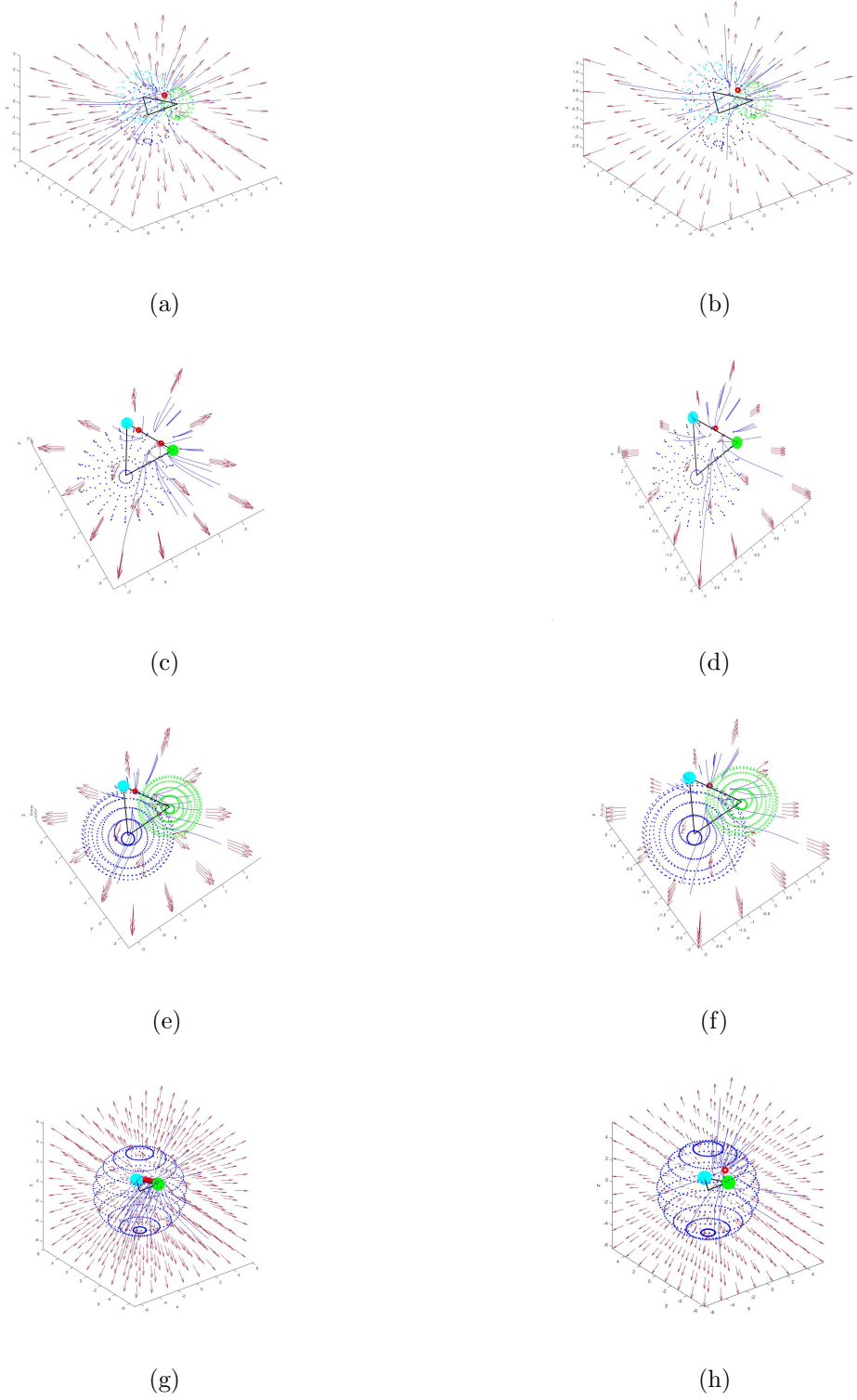


Figure 7: Three-dimensional solution with gradient direction quiver plots when (a,b) $S_{123} \neq \phi$, (c,d) $|T| = 2$, (e,f) $|T| = 1$ and $N_1 \in D_2$, and (g,h) $Y_{100} \cap R_{100} \neq \phi$ with Δ being equilateral. Plots (a,c,e,g) correspond to the distance error case, and plots (b,d,f,h) correspond to the squared distance error case.

distance case. The difference between two- and three- dimensional squared distance cases arises from Lemma 10.

Extending this research to a multi-measruement analysis will be the focus of future works. The existence of multiple potential signal sources adds complexity to the localization process. Accurately distinguishing among these sources and correctly identifying the true one is crucial for ensuring the stability and reliability of the GPS system. This research on source localization with limited measurements aims to resolve potential ambiguities and non-uniqueness in the solutions. A key contribution of this work is the exploration of how these limitations affect the problem and the identification of strategies to mitigate them.

6 Acknowledgements

This paper was supported by the NRF (National Research Foundation of Korea) grant funded by Korean government (Ministry of Science and ICT : RS-2023-00242308).

References

- [1] Kwon K, Uniqueness and nonuniqueness for the L^1 minimization source localization problem with three measurements, *Applied Mathematics and Computation*, **413**(2022) 126649
- [2] Kwon K, Exact solutions for source localization with squared distance error, *Applied Mathematics and Computation* **427**(2022) 127187
- [3] Kwon K, The number of global solutions for GPS source loacalizaiton in two-dimension, *Journal of Mathematics* **2024**(2024) 7980810